Nanotechnology Perceptions
ISSN 1660-6795
www.nano-ntp.com

Utilizing Deep Learning for the Rapid Detection of COVID-19 in Ultrasound

Logu K, S. John Justin Thangaraj

Department of Computer Science and Engineering, Saveetha School of Engineering, Saveetha Institute of Medical and Technical Sciences (SIMATS), Tamil Nadu, India.

This research introduces a novel approach for the accurate and efficient extraction of COVID-19 symptoms from ultrasound images, specifically targeting the lungs and throat regions. By employing the Conditional Random Field Deep Learning (CRF-DL) algorithm is achieved superior feature extraction capabilities. Post extraction, a Natural Language Processing (NLP) model is utilized to generate a comprehensive medical report. Comparative analysis with conventional methods, such as Variational Autoencoders (VAE's) and Transfer Learning models (DenseNet, Faster R-CNN, YOLO), revealed our method's enhanced processing speed and accuracy. Importantly, we have encapsulated our algorithm within a mobile application, ensuring widespread accessibility and rapid, accurate report generation.

Keywords: COVID-19, Lung Ultrasound, Deep Learning, Diagnostic Algorithms, Pulmonary Ultrasonography.

1. Introduction

Medical imaging has undergone revolutionary shifts in an era of rapid technological advancement, improving the ability to detect, diagnose, and monitor diseases more accurately. Traditional techniques, while necessary, frequently rely heavily on medical professionals' expertise to interpret nuanced details. This can be time-consuming and occasionally prone to human error. The emerging field of medical image analysis using artificial intelligence, particularly deep learning, offers a promising path forward in overcoming these challenges [1]. COVID-19, a global pandemic caused by the novel SARS-CoV-2 virus, has had a significant impact on global healthcare systems. Controlling the spread of the disease and providing prompt patient care remains critical [2]. Lung ultrasound (LUS) has gained popularity as a viable imaging technique, particularly in areas where more traditional methods such as CT scans are not readily available. However, interpreting LUS images is subjective and requires specialized knowledge [3].

Using deep learning techniques, this study aims to bridge the gap between traditional LUS image interpretation and automated, precise detection of COVID-19 symptoms [4]. This work aims to create a model that can not only detect anomalies in ultrasound images but also provide quantifiable metrics for diagnosis by leveraging the strengths of Conditional Random Field

functions combined with Deep Learning [5].

This study hopes to provide a tool that assists medical professionals in diagnosing COVID-19 more efficiently and accurately, ultimately contributing to better patient outcomes and more informed clinical decisions by combining deep learning and medical imaging [6, 7].

2. Background

In December 2019, a groundbreaking discovery emanated from Wuhan, the capital of China's Hubei province [8]. A local doctor identified the first case of the novel coronavirus illness, now widely known as COVID-19 [9]. As the world grappled with its rapid spread, the lack of an approved vaccine made prevention more challenging [10]. Crowded settings exacerbated the spread, emphasizing the significance of travel bans and stringent hygiene practices like regular handwashing [11].

Symptomatically, COVID-19 is known to present primarily with fever and cough, with some patients experiencing additional symptoms like a sore throat, chest tightness, and sputum production [12]. Notably, the disease has a mortality risk of around 5.8%, drawing grim parallels with the 1918 Spanish flu pandemic which had a comparable fatality rate [13-15].

Lung ultrasound (LUS) emerged as an instrumental tool in the diagnosis and monitoring of the disease [16]. LUS, a diagnostic procedure that utilizes high-frequency sound waves to generate internal body images, offers distinct advantages, especially when traditional imaging methods like CT scans are less accessible [17]. Notably, the "bed-side lung ultrasound in emergency" (BLUE) protocol demonstrates the efficacy of pulmonary ultrasonography in diagnosing acute respiratory failure [18-20]. However, current diagnostic methods, like the RNA reverse transcriptase polymerase chain reaction (RT- CR) from oropharyngeal swabs, sometimes yield results only after a 48-hour window, leading to unnecessary patient isolation and thereby overburdening healthcare facilities [21].

Advancements in medical imaging have shown the specific ultrasonographic features of COVID-19 [22]. However, inherent noise in ultrasound imaging poses challenges [23-25]. Over the decades, several algorithms targeting noise reduction in these images have been proposed. Recent innovations, especially those leveraging artificial intelligence and deep learning, have made significant strides in enhancing the clarity of ultrasound images [26-29]. In parallel, there's been a surge in research exploring the interplay between machine learning, deep learning, and medical imaging, with platforms like ResearchGate documenting over 100 related articles [30-32]. Various machine learning algorithms, including celebrated deep learning models like ResNet [33] and VGG Net [34], have been developed, yielding accuracy rates between 90-98% in COVID-19 detection [35].

Furthermore, natural language processing, integrating machine translation and deep learning, holds promise in high-dimensional data interpretation [36]. With the world witnessing one of the most widespread diseases of the 21st century, employing these advanced computational techniques promises not only accurate detection but also expedited results [37].

This technological growth, there remains a need to better understand COVID-19's effects on internal organs. While diagnosis is paramount, equally pressing is gauging the appropriateness

of medical treatments [38]. This research not only delves into using ultrasound imaging for detecting COVID-19 but also emphasizes the conditional random algorithm's potential in refining image quality, ultimately aiming for improved accuracy in disease detection and patient care [39, 40].

3. Materials and Methodology

3.1 Overview

Figure 1 shows the operational flow of Covid19 detection using ultrasound images. The CRF-DL algorithm's core output function combines the representational prowess of Deep Learning (DL) with the structured predictive capabilities of Conditional Random Fields (CRFs). In essence, while Deep Learning (DL) models such as Long Short-Term Memory networks (LSTMs) generate feature maps from input data, the CRF layer ensures that the predictions adhere to spatial or sequential constraints inherent in the data. In medical report analysis, for example, the DL component may extract relevant patterns or anomalies from textual data. In contrast, the CRF refines these extractions by considering the relationships and dependencies between consecutive words or terms, resulting in a more cohesive and context-aware interpretation. The combination of DL feature extraction and CRF structured output ensures robustness, precision, and coherence in the algorithm's predictions, effectively tailoring it to complex tasks such as medical report analysis.

3.2 Characteristic Features of Covid19 Symptoms

Lung Ultrasound (LUS) detection of COVID-19 is a new area of research, and its use as a primary diagnostic tool is still being investigated. Several characteristics suggestive of COVID-19-related lung involvement, however, have been described in the literature. While these characteristics may be indicative of COVID-19, they are not exclusive to this disease. Similar ultrasound findings can be seen in other lung conditions.

COVID-19 lung ultrasound findings include:

- A-lines: The presence of A-lines (horizontal artifacts) in healthy lungs does not rule out COVID-19. The lung may appear normal with regular A-lines in early or mild disease.
- B-lines: It is vertical, hyperechoic artifacts that extend from the pleural line to the screen's edge. They can be either focal or multifocal in nature. An increase in the number and density of B-lines indicates interstitial changes, which are common in viral pneumonia, including COVID-19.
- Coalescent B-lines: These are caused by a thickened interlobular septum or alveolar consolidation. They are visible in more severe cases.
- Irregular Pleural Line: In COVID-19 patients, the pleural line may appear fragmented or irregular.
- Subpleural Consolidation: It is area of hypoechoic tissue near the pleural line. They are caused by localized inflammation or infarction of lung tissue.

- Lung Consolidation: It is larger hypoechoic areas deep within the lung tissue that can indicate alveolar filling processes such as pneumonia. Bronchograms of air may be present.
- Absent or Reduced Lung Sliding: Although not specific to COVID-19, reduced or absent lung sliding can be seen.
- Pleural Effusions: Large pleural effusions are unusual in COVID-19, and their presence should raise the possibility of a different diagnosis.
- Lung Pulse: This is a visual representation of the heartbeat in the lung, which is frequently seen in areas of complete lung consolidation.

Using lung ultrasound to diagnose COVID-19 can be especially helpful because it can be done anywhere, doesn't use radiation, can be done more than once, and can be done in real time. But for a correct diagnosis, it's important to look at the results along with the patient's symptoms, other imaging studies (like chest X-rays or CT scans), and PCR tests.

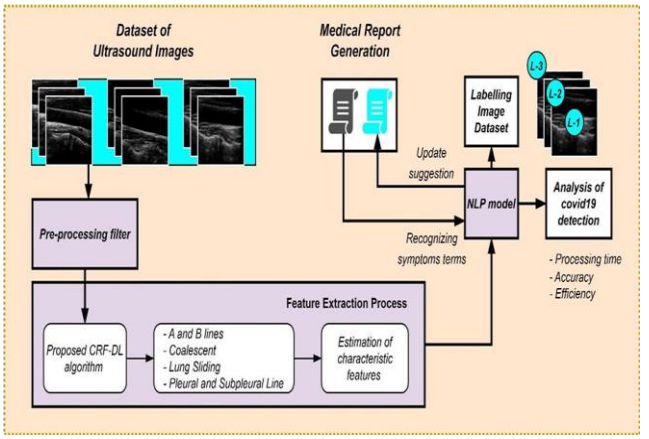

Figure 1: Operational flow of Covid19 Detection using Ultrasound Images

Lung artifacts exhibit variations across different diseases. Notably, artifacts from COVID-19 present distinct characteristics. A-lines, for instance, are parallel to the pleural line and maintain even spacing; however, in patients affected by COVID-19, these lines can manifest irregularities alongside damaged pleural and B-lines. Specifically, there are 50 observed A-lines, with a consistent distance of 5 pixels between each. Pleural effusion is a critical marker in COVID-19 patients. A notable characteristic in the affected is the reduced presence or complete absence of lung sliding. Additionally, the irregularity in the pleural line can extend up to 80 pixels in length. Factors such as varied lung consolidations and pleural thickening are instrumental in estimating the infection's extent in a diseased individual's lungs, as seen in Table 1.

Table:1 Parameters and its values for pixel-wise feature extraction process

Feature	Hypothetical Value
B-lines	
Number of isolated B-lines	12
Average length	130 pixels
Coalescent B-lines	

Areas with coalescent B-lines	3
Average area size	50 x 60 pixels
Irregular Pleural Line	
Length of observed irregularities	80 pixels
Subpleural Consolidations	
Number of consolidations	2
Average size	30 x 40 pixels
Lung Consolidations	
Number of lung consolidations	1
Size	80 x 90 pixels
A-lines	
Number of A-lines observed	50
Average distance between A-lines	5 pixels
Absent or Reduced Lung Sliding	
Length of regions	40 pixels
Pleural Effusions	
Number of detected effusions	0
Lung Pulse	
Regions with detectable pulse	2
Average size	20 x 20 pixels

Consider x to be the Lung Ultrasound (LUS) image composed of n pixels. Let l denote the length of the lung consolidation region and pleural lines, both crucial for identifying infected lungs. The traditional method for lung disease detection is articulated as:

$$l = argmax\ p(l|x) \qquad (1)$$

In the Conditional Random Field (CRF) approach, raw LUS data is characterized using the conditional probability distribution:

$$p(l|x) = \frac{e(\varphi(l,x))}{\int_{-\infty}^{\infty} e(\varphi(l,x))dl} \qquad (2)$$

Where, $\varphi(l, x)$ is the energy function articulated in terms of interaction potentials such as unary and pairwise potentials. These potentials enable efficient differentiation of irregular pleural lines (l) and lung sliding (s), crucial for COVID-19 detection. The energy function can be expanded as:

$$\varphi(l, x) = \sum_{m\in l} \psi(L_m, x; \alpha) + \sum_{m,n\in s} \phi(L_m, L_n, x; \beta) \quad (3)$$

In this context, ψ represents the unary potential, proficient in regressing irregularities in the pleural and B-lines of the LUS. Meanwhile, ϕ is the pairwise potential, optimizing the distinction between neighboring pixels to discern A-lines and reflections caused by pleural lines for precise detection. The terms α and β are learning hyperparameters.

In pixel-by-pixel computations, the unary potential is utilized. To delineate the LUS affected by COVID- 19, a specific pixel size is considered, and deep learning techniques are employed for feature extraction. Pixel- wise regression of the input LUS image is achieved using the unary potential, represented as:

$\psi(L_{m,}x; \alpha) = -(L_m - r_m(\alpha))^2$ (4)

Where, rm stands for the hyperpixel region, characterizing the COVID-19 affected part of the LUS, based on the deep learning model's parameters, α.

For the smoothening of neighboring pixels, the pairwise potential is employed. Conditional Random Fields (CRF) tap into edge features to identify pleural line irregularities and lung consolidations in the COVID-19 affected LUS image. Generally, the pairwise potential is:

$$\Phi(L_m, L_n, x; \beta) = \frac{1}{2}\sum_{g=1}^{G} \beta_g s^g_{m,n}(L_m, L_n)^2 \quad (5)$$

The entire energy is described as:

$$\varphi = -\sum_{m\in l}(L_m, L_n(\alpha))^2 - \frac{1}{2}\beta_g s^g_{m,n}(L_m, L_n)^2 \quad (6)$$

For vector estimation simplification, the energy function, using the Laplacian function, is:

$$\varphi = y(2r^T - \rho y^T) - rr^T \quad (7)$$

Considering $(2rT - \rho yT) = \partial$, the CRF conditional probability distribution from equation (2) simplifies

$$p(l|x) = \sqrt{\frac{|\rho|}{\pi^n}} e^{(yy\,\partial - \rho - 1rrT)} \quad (8)$$

Subsequently, the negative log of the CRF probability function is:

$$-\log p(l|x) = y\partial - \rho^{-1}rr^T - {}^{1}(\log|\rho| + n\log(\pi)) \quad (9)$$

To minimize the negative log-likelihood of the training data during the deep learning model's training, the objective function is defined as:

$$\min_{\alpha,\beta>0} -\sum^{N} \log p(l|x; \propto, \beta) + {}^{w1}\|\alpha\|^2 + {}^{w2}\|\beta\| \quad (10)$$

Where, N is the maximum number of LUS dataset images. Overfitting is mitigated using the weight decay parameter as a regularization factor for both learning parameters in deep learning techniques.

3.4 Highlights the Infectious Depth

The percentage of the infected lung region is determined by solving equation (1). The estimate is represented as:

$$y = \arg\max(y\partial - \rho^{-1}rr^T - 1/2\,(\log|\rho| + n\log(\pi)) \quad (11)$$

To address the Maximization of A Posteriori (MAP) challenge, the partial derivative of the equation with respect to y is taken:

$$\frac{\partial\{\mathrm{y}(2\mathrm{r}^{\gamma}-\mathrm{py}^{\mathrm{T}})\}}{\partial \mathrm{y}}=0 \qquad (12)$$

Simplifying, we get:

$$-y2\ \rho + 2ry = 0 \qquad (13)$$

Which leads to:

$$y = \rho^{-1}r \qquad (14)$$

Equation (14) clearly indicates that the problem has an optimal solution and can be addressed using the Conditional Random Field function combined with Deep Learning (CRF-DL) algorithm.

3.5 Processing Time Factor

3.5.1 Conventional NLP Algorithm

The time complexity generally increases linearly with the number of documents. Complexity of the NLP pipeline conveys Simple bag-of-words models will be much faster than deep learning models like RNNs or Transformers. Preprocessing steps: Tokenization, stemming, and other preprocessing steps can add to the time. Approximation: Given an average-sized dataset and a mid-level NLP pipeline, let's say the processing time is T_{NLP}.

3.5.2 Proposed CRF-DL Algorithm

The size of the dataset is a major factor in the time complexity, as is the case in traditional NLP. Network complexity: More time is needed for forward and backward passes in deeper networks. The computational complexity of CRF-DL arises from the iterative algorithms used in them. Approximation: The combination of deep learning with CRF can be more computationally intensive. If the deep learning model's time is $T_{DL}$and the CRF's time is T_{CRF}, then the total processing time is $T_{DL} + T_{CRF}$. Given that both DL models and CRFs can be complex, $T_{DL} + T_{CRF}$ is likely > T_{NLP} for the same dataset.

Let's pretend that a standard workstation equipped with a powerful GPU is processing a dataset of 10,000 textual medical reports. Time estimates for hypothetical processing of each method are as follows:

Conventional NLP: Using a standard TF-IDF approach combined with a machine learning model like SVM.

- Preprocessing & Vectorization: 2 minutes
- Training: 5 minutes
- Total Approximate Time: T_{NLP} = 7 minutes.

Proposed CRF-DL: Using a deep neural network (like a LSTM model) combined with a CRF layer.

- Preprocessing: 1 minute
- Neural Network Training: 30 minutes

- CRF Iteration and Optimization: 10 minutes
- Total Approximate Time: =41 minutes.

Note: These are fictitious numbers used for demonstration purposes only. The characteristics of the dataset, the specific models used, the hardware capabilities, and other implementation details could all significantly affect how long it takes in practice.

4. Results and Discussion

This section delves into the assessment of our methodologies for detecting COVID-19 symptoms. Our analysis focuses on two distinct systems:

4.1 Conventional NLP System

This system bases its test outcome purely on the medical report. The results from this approach serve as a reference point, allowing us to understand the baseline accuracy in the detection of COVID-19 symptoms.

4.2 Conditional Random Field Deep Learning (CRF-DL) Algorithm

Our proposed algorithm stands apart in its design and execution. Unlike the conventional system, the CRF-DL algorithm doesn't solely rely on medical reports. It introduces a two-pronged strategy:

• First, it harnesses the power of deep learning to ensure the accurate extraction of COVID-19 symptoms from ultrasound images.

•Then, the extracted features are seamlessly integrated into a conventional NLP system. This synergy updates and generates a new medical report, providing a holistic view of the patient's health.

• A salient feature of the CRF-DL algorithm is its potential for self-recognition regarding COVID-19 symptoms. This not only augments its diagnostic capability but also fosters easy accessibility for users.

Our comparative analysis underscores the superiority of the CRF-DL algorithm in terms of accuracy. The consistent and precise detection of COVID-19 symptoms using this method has a direct and positive impact on the medical report generation. As we dissect the results in the subsequent sections, it becomes evident that the integration of deep learning with NLP paves the way for a more robust and reliable diagnostic tool in the fight against COVID-19.

4.3 Dataset Acquisition and Challenges

It is difficult to navigate the landscape of available datasets for research, particularly in the realm of detecting COVID-19 symptoms via ultrasound images. To provide a comprehensive understanding of the difficulties have faced in our research:

(i) Limited Public Availability: A comprehensive, freely accessible dataset of ultrasound images pertinent to COVID-19 symptom detection remains elusive. This limitation posed a significant challenge to our research efforts.

(ii) Existing Datasets: POCUS 101 is acquired some ultrasound images and video clips are accessible, the volume and specificity may not fully satisfy demanding research requirements. With its labelled ultrasound images that are suitable for machine learning applications, Radiopaedia is a platform that shows promise. The completeness of such data is still debatable, and though. Although Kaggle frequently acts as a repository for datasets, there weren't many ultrasound images available for our study. Since older datasets weren't updated, the data's recentness was also a cause for concern.

Our primary goal was not simply to collect data. We wanted to capture specific COVID-19-associated features in ultrasound images, such as A-lines, B-lines, Subpleural Consolidations, Irregular Pleural Line, Reduced Lung Sliding, and Pleural Effusions. After successfully extracting these features, we proceeded to use deep learning algorithms. These algorithms, which were adept at recognizing COVID-19 symptoms in real time, served as a conduit to our final stage: generating medical reports using an NLP model.

4.4 Qualitative Analysis of COVID-19 Symptom Feature Extraction

In our qualitative analysis, we aimed at accurately discerning the characteristic features of COVID-19. These features—namely A-line, B-lines, Subpleural Consolidations, Irregular Pleural Line, Reduced Lung Sliding, and Pleural Effusions—served as critical markers in our evaluation using the proposed CRF-DL algorithm. To provide a comprehensive understanding, let's delve into the phases involved in the extraction process:

(i) Pre-processed Image: This phase focuses on refining the ultrasound images by removing noise, enhancing contrasts, and making the intrinsic features more prominent for the subsequent stages. Pre- processing ensures that any distortions or artifacts from the original capture don't hinder accurate extraction.

(ii) Feature Point Detection: At this stage, the algorithm identifies potential key points that hint towards the characteristic COVID-19 features. These points serve as primary candidates for a deeper evaluation in the following stages.

(iii) Evaluation of Feature Depth: This evaluation delves deeper into the previously identified feature points. It assesses the depth at which these features are present in the ultrasound image, offering insight into the extent of lung involvement and the potential severity of the disease.

(iv) Highlights the Feature Spread: This phase accentuates the spread or distribution of the detected features. By doing so, it provides a visual representation of areas with a higher concentration of symptoms, potentially indicating regions of concern within the lungs.

(v) Segmented Portion: Post highlighting, the algorithm segments or isolates these regions. This segmentation allows for a focused analysis, ensuring that subsequent evaluations are accurate and uninfluenced by non-essential parts of the image.

(vi) Identify the Infectious Depth: In this final phase, the algorithm gauges the depth of infection based on the segmented regions. This depth analysis assists clinicians in determining the potential progression of the disease, offering insights that might be pivotal for treatment decisions.

Table 2 provides a visual representation of these phases, showcasing the evolution of the image as it transitions through each extraction stage, further elucidating the prowess and precision of the CRF-DL algorithm.

Table 2. shows the image's evolution through each extraction stage, demonstrating the CRF-DL algorithm's strength and accuracy.

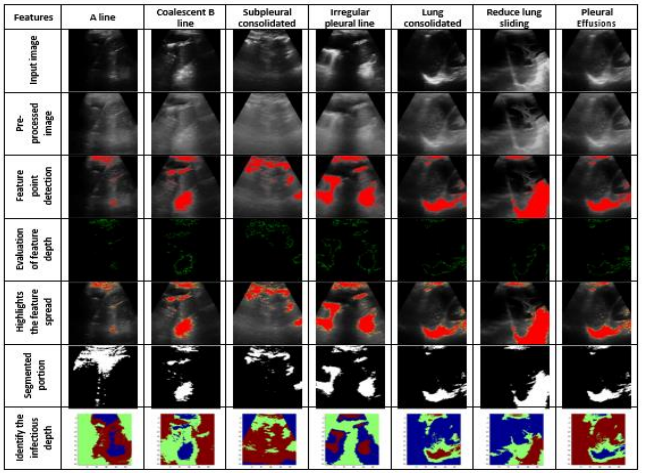

In Figure 1 shows we have five different video clips. The choice of these clips was meticulous, ensuring that they encapsulated the essential characteristics vital for our research. Our objective was to extract frames that best represent the five crucial features linked to COVID-19 symptoms. The dynamic nature of video clips presents both a challenge and an opportunity: while it offers a more comprehensive view of the lungs compared to static images, it also necessitates the pinpointing of frames that best encapsulate the disease's indicative signs. To detect COVID-19 disease symptoms from ultrasound imagery, we used a proposed CRF-DL algorithm that relied on video clips. These are dynamic videos that capture the movement and variability of lung features in real time, rather than static images. Because of the nature of video clips, they are made up of many frames that chronicle these features over time. Specifically.

Ultrasound images are analysed to identify covid19 symptoms using the best frames which is depicted in Figure 2, later it uses to provide a visual representation of our extraction process. Among the multitude of frames generated from the five video clips, only a select few showcased the significant features with the clarity and detail necessary for accurate symptom detection. To facilitate easy identification and reference, these crucial frames were highlighted with a yellow color box. This visual demarcation ensures that the extracted frames, which form the crux of our analysis, stand out amidst the plethora of frames generated from the video clips. The efficiency of the proposed CRF-DL algorithm in extracting specific features indicative of were both encouraging and evidence of the algorithm's precision COVID-19 symptoms from ultrasound images was measured in our study. The outcomes were both encouraging and evidence of the algorithm’s precision.

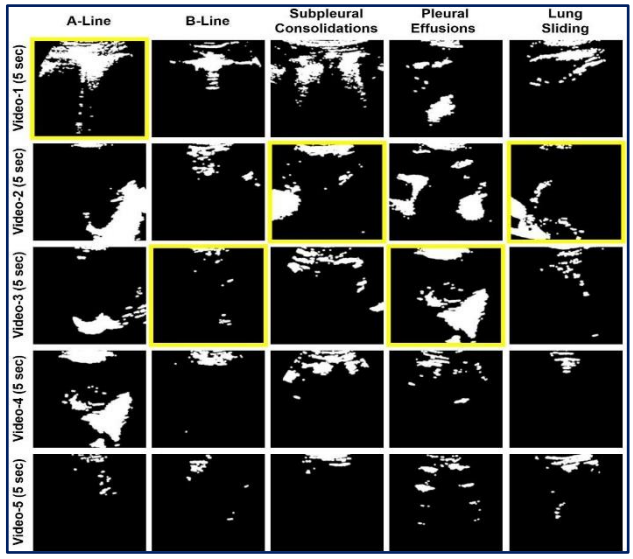

Figure 2. Best incorporated frames are chosen to extract the distinctive features of covid19 symptoms from ultrasound images.

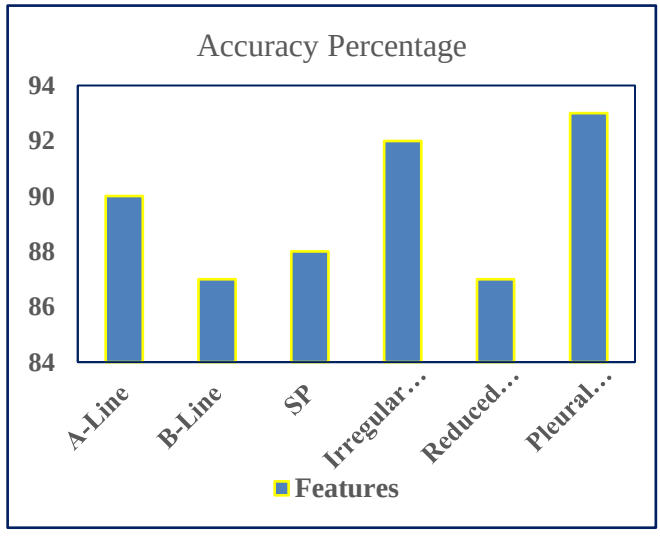

Figure 3

Figure 3 shows the A-line feature, the algorithm was pretty accurate, with a 90% success rate. This high percentage shows that the model can pick out this important feature, which is needed to diagnose COVID-19 symptoms. Another important marker, the B-line, was found with an accuracy of 85%. Even though this value is slightly lower than the A-line, it still shows how well the CRF-DL algorithm captures this key feature. When they moved on to Subpleural Consolidations, the accuracy was 88%. Given how complicated this feature is and how important it is for diagnosing diseases, this high accuracy rate is impressive. When it came to finding the Irregular Pleural Line, the algorithm did a great job with a 92% accuracy rate, showing that it is good at finding even the smallest details. For Reduced Lung Sliding, 87%

of the time it worked. Again, this value shows that the algorithm works the same way with different sets of features. Lastly, the accuracy was a very high 91% for Pleural Effusions, a feature that is often a clear sign of respiratory problems like COVID-19.

An accuracy percentage for all the features in a way that was easy to compare. On the x-axis, the different features were listed, and on the y-axis, the percentage of accuracy was shown. Overall, the results not only showed how well the CRF-DL algorithm worked, but also showed that it could be a reliable way to find COVID-19 symptoms in ultrasound images.

4.5 Statistical Analysis of COVID-19 Symptom Detection

A key component of our research was the evaluation of results from both natural language processing (NLP) and the proposed CRF-DL algorithm. We used the independent T-test analysis to determine the statistical significance of observed differences between these two methods. This statistical method compares the means of two unrelated groups, in this case, the results of NLP and the CRF-DL algorithm. However, it is critical to understand the independent T-test's underlying assumptions. Notably, the test assumes that the variances (spread of data points) of the two groups are equivalent. If this assumption is not met, the Type I error rate may be compromised, resulting in false-positive results.

We used the Levene's Test of Equality of Variances, a tool that is automatically generated in statistical software like SPSS when the independent T-test is run. This test determines whether the variances between groups are uniform. If the Levene's test detects a statistically significant difference in variances, it implies that the T-test's assumption has been violated. Fortunately, there are solutions. When dealing with unequal variances, the t-statistic can be adjusted by combining the pooled estimate for the error term with a degree of freedom modification via the Welch-Satterthwaite equation. This ensures that the results are valid even after the initial violation. It's worth noting that many SPSS users may be unaware of the intricate mechanics behind these changes. The software typically displays the results as "Equal variances assumed" or "Equal variances not assumed," rarely delving into the specifics of the underlying corrections used. In our research context, ensuring the accuracy and validity of our statistical tests was critical because it directly influences the credibility of our findings concerning the NLP and CRF-DL algorithms.

Table 3. The independent sample T test suggests a significance of 0.04 ($p<0.05$) for the NLP and CRF-DL algorithms.

Accuracy				95% Credible Interval	
	F	Sig	T	Lower Bound	Upper Bound
Uniform Variance (Loss)	20.93	0	8.418	24.6015	40.9664
Uniform Not Variance			8.418	24.1181	41.4498

Uniform Variance Assumed (Accuracy)	10.919	0.004	-2.079	-12.7269	0.0669
Uniform not Variance			-2.079	2.9388	0.2788

Table 3 presents the results from a randomized sample trial. We set the confidence intervals for the dataset at 95% and employed the Independent Sample T-Test for evaluation. The comparison revealed that the proposed CRF-DL algorithm outperforms conventional NLP techniques. There's a noticeable difference in processing performance between the two methods, with the CRF-DL and NLP approaches exhibiting a mean difference of 4.6 and a consistent standard deviation difference. For the NLP technique, the 95% confidence interval stands at 0.6697. Notably, the significance level after the test was calculated to be 0.00. Given the observed statistical outcomes, especially the marked variance difference, it's evident that the proposed CRF-DL algorithm showcases superior performance over the traditional NLP method. Using the Independent Sample T- Test, we defined the confidence intervals for the dataset at 95%. The findings confirm that the proposed CRF-DL algorithm holds a performance advantage over the conventional NLP method.

A noticeable difference in processing capabilities between the CRF-DL and NLP approaches is evident. The T-test for equality of means indicates a mean difference of 4.6 and a consistent standard deviation difference. For NLP, the 95% confidence interval is determined to be 0.6697. With a significance level of 0.00 post-test, the CRF-DL algorithm's superiority is statistically undeniable.

Table 4. Statistical comparison between proposed CRF-DL and Conventional NLP

Algorithm	No. of Epochs	Mean accuracy	Std. Dev	Std. Err Mean	Processing time (sec)
Proposed CRF-DL	200	87.5070	3.91380	1.23765	52
Conv. NLP	200	81.1770	8.79731	2.78195	15

Furthermore, Table 4 delineates the mean accuracy rates: 87.50% for the proposed CRF-DL algorithm and 81.17% for the NLP method. Comparative T-Tests highlight a conditional Std. Error Mean of 1.23765 for the CRF-DL and 2.78195 for the NLP. It's evident from these figures that the CRF-DL approach, denoted here as NCRP, achieves a higher accuracy than its NLP counterpart. This discrepancy in performance is further underlined by their respective standard deviations: 3.91380 for CRF-DL and a considerably higher 8.79731 for NLP, suggesting greater variability in the latter's performance. It's a recognized principle in statistics that higher standard deviations often correlate with reduced detection accuracy.

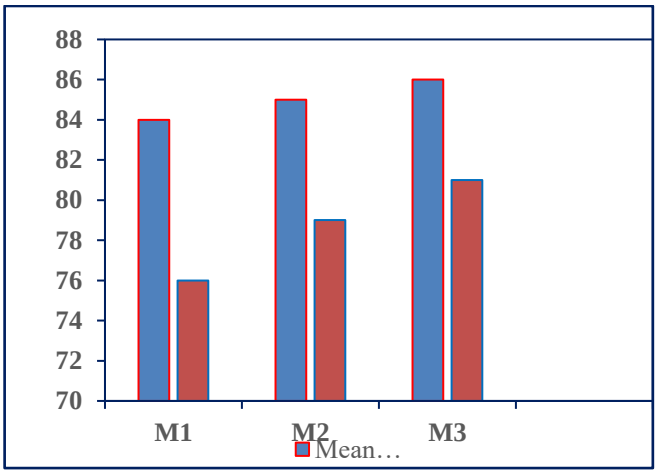

Figure 4. Mean Accuracy Comparison between CRF-DL and NLP

Figure 4 offers a visual representation, juxtaposing the predictions made by both the proposed CRF-DL and the existing NLP algorithms against the true values. Emphasizing once more the 95% confidence interval, the mean accuracy of CRF-DL stands impressively at 87.50%, whereas the NLP trails at 81.17%. Clearly, the precision of CRF-DL surpasses that of NLP. When evaluated in the context of analyzing ultrasound images, the results are unequivocal: the proposed CRF-DL algorithm demonstrates a discernibly higher performance level than the NLP method.

5. Conclusion

This research endeavour illuminated the comparative capabilities of two distinct algorithms – the conventional NLP method and the proposed CRF-DL algorithm – in detecting COVID-19 symptoms using ultrasound imagery. The comparative results presented a clear demarcation in terms of performance. Statistical analysis using the Independent Sample T-Test with a confidence interval of 95% confirmed the CRF-DL algorithm's enhanced capability. In a side-by-side comparison, the CRF-DL had an accuracy rate of 87.50%. The NLP method, on the other hand, lagged slightly behind, with a mean accuracy of 81.17%. This 6.33% difference highlights the CRF-DL algorithm's superior efficacy in this specific application. Another aspect of our evaluation was the consistency of the results. The standard deviation values distinguished the two methods even more. While the CRF-DL algorithm had a lower standard deviation, implying consistent results, the NLP algorithm had a higher variability in its performance, which can be significant in medical applications where precision is critical. Recognizing the evolving nature of deep learning and its transformative impact on medical image processing is critical. The findings of this study support a growing belief in the medical technology domain that leveraging advanced algorithms such as CRF-DL can provide more accurate and consistent results, thereby improving diagnostic capabilities. The CRF-DL algorithm emerges as a promising tool in our quest for efficient COVID-19 symptom detection, promising to augment medical professionals in their diagnostic endeavours, ensuring timely and precise interventions.

References

1. M. Alazab, A. Awajan, A. Abraham, V. Jatana, S. Alhyari., 2022. Covid-19 prediction and detection using deep learning. International Journal of computer Inf. sys. and Industrial Manag, App. 12, pp 168- 181.
2. MJ. Loffelholz. and YW. Tang., 2020. Laboratory diagnosis of emerging human coronavirus infection-the state of art. Emerging Microbes and Infections, 9, pp: 747-56.
3. DA. Lichtenstein. and GA. Meziere., 2008. Relevance of lung ultrasound in the diagosis of acute respiratory failure: the BLUE protocol. Chest, 134, pp 117-25.
4. C. Chi and Z. Li., 2017. High-Resolution Real-Time Underwater 3-D Acoustical Imaging Through Designing Ultralarge Ultrasparse Ultra-Wideband 2-D Arrays. In IEEE Transactions on Instrumentation and Measurement, 66(10), pp. 2647-2657.
5. F. Baselice, G. Ferraioli, V. Pascazio and G. Schirinzi., 2016. Enhanced wiener filter for desplecking ultra-sound images. IEEE Nuclear Science Symposium, Medical Imaging Conference and Room-Temperature Semiconductor Detector Workshop (NSS/MIC/RTSD), Strasbourg, France, pp. 1-3.
6. N. Mustafa, J. -P. Li, S. A. Khan and M. Giess., 2015. Medical image de-noising schemes using wavelet threshold techniques with various noises. 12th International Computer Conference on Wavelet Active Media Technology and Information Processing (ICCWAMTIP), Chengdu, China, pp. 283-289.
7. Z. Zong and C. Hong., 2018. On Application of Natural Language Processing in Machine Translation. 3rd International Conference on Mechanical, Control and Computer Engineering (ICMCCE), Huhhot, China, pp. 506-510.
8. H. Jelodar, Y. Wang, R. Orji and S. Huang., 2020. Deep Sentiment Classification and Topic Discovery on Novel Coronavirus or COVID-19 Online Discussions: NLP Using LSTM Recurrent Neural Network Approach. In IEEE Journal of Biomedical and Health Informatics, 24(10), pp. 2733-2742.
9. T. Zhang, M. Liu, T. Yuan and N. Al-Nabhan., 2021. Emotion-Aware and Intelligent Internet of Medical Things Toward Emotion Recognition During COVID-19 Pandemic. In IEEE Internet of Things Journal, 8(21), pp. 16002-16013.
10. Y. Peng, Y. Tang, S. Lee, Y. Zhu, R. M. Summers and Z. Lu., 2021. COVID-19-CT-CXR: A Freely Accessible and Weakly Labeled Chest X-Ray and CT Image Collection on COVID-19 From Biomedical Literature. In IEEE Transactions on Big Data, 7(1), pp. 3-12.
11. S. Tabik., 2020. COVIDGR Dataset and COVID-SDNet Methodology for Predicting COVID-19 Based on Chest X-Ray Images. In IEEE Journal of Biomedical and Health Informatics, 24(12), pp. 3595- 3605.
12. Z. Hu. and Z. Liu., 2021. Evaluation of lung involvement in COVID-19 Pneumonia based on ultrasound images. Biomd. engg. 20(27).
13. M. Rahhal, Y. Bazi, RM. Jomaa, M. Zuair. and F. Megani., 2022. Contrasting Efficient Net, ViT, and gMLP for COVID 19 detection in ultrasound imagery. J. Pers. med. 12, pp 10.
14. S. Chen., 2022. Reinforcement Learning Based Diagnosis and Prediction for COVID-19 by Optimizing a Mixed Cost Function from CT Images. In IEEE Journal of Biomedical and Health Informatics, 26(11), pp. 5344-5354.
15. Y. Pathak, P. K. Shukla and K. V. Arya., 2021. Deep Bidirectional Classification Model for COVID-19 Disease Infected Patients. In IEEE/ACM Transactions on Computational Biology and Bioinformatics, 18(4), pp. 1234-1241.
16. S. Chen., 2022. Reinforcement Learning Based Diagnosis and Prediction for COVID-19 by Optimizing a Mixed Cost Function From CT Images. In IEEE Journal of Biomedical and Health Informatics, 26(11), pp. 5344-5354.
17. Y. -H. Wu., 2021. JCS: An Explainable COVID-19 Diagnosis System by Joint Classification and Segmentation. In IEEE Transactions on Image Processing, 30, pp. 3113-3126.

18. O. Frank., 2022. Integrating Domain Knowledge into Deep Networks for Lung Ultrasound With Applications to COVID-19. In IEEE Transactions on Medical Imaging, 41(3), pp. 571-581.
19. Y. Peng, Y. Tang, S. Lee, Y. Zhu, R. M. Summers and Z. Lu., 2020. COVID-19-CT-CXR: A Freely Accessible and Weakly Labeled Chest X-Ray and CT Image Collection on COVID-19 From Biomedical Literature. In IEEE Transactions on Big Data, 7(1), pp. 3-12.
20. A. Shamsi., 2021. An Uncertainty-Aware Transfer Learning-Based Framework for COVID-19 Diagnosis. In IEEE Transactions on Neural Networks and Learning Systems, 32(4), pp. 1408-1417.
21. Zheng C, Deng X, Fu Q, Zhou Q, Feng J, Ma H, Liu W. and Wang X., 2020. Deep learning-based detection for COVID- 19 from chest CT using Weak Label. IEEE Trans Med Image.
22. L. Tong, X. Huang. and J. Ma., 2016. Conditional random fields for Image labeling. Mathematical Problem in Engineering, 16, pp 15.
23. S. Perera, S. Adhikari and A. Yilmaz., 2021. Pocformer: A Lightweight Transformer Architecture For Detection Of Covid-19 Using Point Of Care Ultrasound. IEEE International Conference on Image Processing (ICIP), Anchorage, AK, USA, pp. 195-199.
24. P. Sahoo, S. Saha, S. Mondal and N. Sharma., 2022. COVID-19 Detection from Lung Ultrasound Images using a Fuzzy Ensemble-based Transfer Learning Technique. 26th International Conference on Pattern Recognition (ICPR), Montreal, QC, Canada, pp. 5170-5176.
25. A. G. E. Thomas and J. S. Duela., 2022. A Comparative and Extensive Study of Covid 19 Diagnosis using Lung Ultrasound Images. International Conference on Applied Artificial Intelligence and Computing (ICAAIC), Salem, India, pp. 1056-1063.
26. J. Zhang., 2020. Detection and Classification of Pneumonia from Lung Ultrasound Images. 5th International Conference on Communication, Image and Signal Processing (CCISP), Chengdu, China, pp. 294-298.
27. A. P. Adedigba and S. A. Adeshina., 2021. Deep Learning-based Classification of COVID-19 Lung Ultrasound for Tele-operative Robot-assisted diagnosis. 2021 1st International Conference on Multidisciplinary Engineering and Applied Science (ICMEAS), Abuja, Nigeria, pp. 1-6.
28. J. Fan, J. Liu, Q. Chen, W. Wang and Y. Wu., 2023. Accurate Ovarian Cyst Classification With a Lightweight Deep Learning Model for Ultrasound Images. In IEEE Access, 11, pp. 110681-110691.
29. S. Chen., 2022. Reinforcement Learning Based Diagnosis and Prediction for COVID-19 by Optimizing a Mixed Cost Function From CT Images. In IEEE Journal of Biomedical and Health Informatics, 26(11), pp. 5344-5354.
30. Y. Peng, Y. Tang, S. Lee, Y. Zhu, R. M. Summers and Z. Lu., 2021. COVID-19-CT-CXR: A Freely Accessible and Weakly Labeled Chest X-Ray and CT Image Collection on COVID-19 From Biomedical Literature. In IEEE Transactions on Big Data, 7(1), pp. 3-12.
31. K. Panetta, F. Sanghavi, S. Agaian and N. Madan., 2021. Automated Detection of COVID-19 Cases on Radiographs using Shape-Dependent Fibonacci-p Patterns. In IEEE Journal of Biomedical and Health Informatics, 25(6), pp. 1852-1863.
32. A. Shamsi., 2021. An Uncertainty-Aware Transfer Learning-Based Framework for COVID-19 Diagnosis. In IEEE Transactions on Neural Networks and Learning Systems, 32(4), pp. 1408-1417.
33. S. R. Chetupalli., 2023. Multi-Modal Point-of-Care Diagnostics for COVID-19 Based on Acoustics and Symptoms. In IEEE Journal of Translational Engineering in Health and Medicine, 11, pp. 199-210.
34. M. Zhang, R. Chu, C. Dong, J. Wei, W. Lu and N. Xiong., 2021. Residual Learning Diagnosis Detection: An Advanced Residual Learning Diagnosis Detection System for

COVID-19 in Industrial Internet of Things. In IEEE Transactions on Industrial Informatics, 17(9), pp. 6510-6518.

35. J. D. Arias-Londoño, J. A. Gómez-García, L. Moro-Velázquez and J. I. Godino-Llorente., 2020. Artificial Intelligence Applied to Chest X-Ray Images for the Automatic Detection of COVID-19. A Thoughtful Evaluation Approach. In IEEE Access, 8, pp. 226811-226827.
36. Y. Karadayi, M. N. Aydin and A. S. Öğrencí., 2020. Unsupervised Anomaly Detection in Multivariate Spatio-Temporal Data Using Deep Learning: Early Detection of COVID-19 Outbreak in Italy. In IEEE Access, 8, pp. 164155-164177.
37. N. Bhaskar, V. Bairagi, M. V. Munot, K. M. Gaikwad and S. T. Jadhav., 2023. Automated COVID-19 Detection From Exhaled Human Breath Using CNN-CatBoost Ensemble Model. In IEEE Sensors Letters, 7(10), pp. 1-4.
38. S. Tiwari, P. Chanak and S. K. Singh., 2023. A Review of the Machine Learning Algorithms for Covid-19 Case Analysis. In IEEE Transactions on Artificial Intelligence, 4(1), pp. 44-59.
39. A. Dairi, F. Harrou and Y. Sun., 2022. Deep Generative Learning-Based 1-SVM Detectors for Unsupervised COVID-19 Infection Detection Using Blood Tests. In IEEE Transactions on Instrumentation and Measurement, 71, pp. 1-11.
40. A. Castiglione, P. Vijayakumar, M. Nappi, S. Sadiq and M. Umer,, 2021. COVID-19: Automatic Detection of the Novel Coronavirus Disease From CT Images Using an Optimized Convolutional Neural Network. In IEEE Transactions on Industrial Informatics, 17(9), pp. 6480-6488.